The Radiation Environment for the Change-out Scenarios of the SNS Inner Plug and the Proton Beam Window Insert

Franz X. Gallmeier and Igor Remec

Oak Ridge National Laboratory
P.O. Box 2008, MS6474
Oak Ridge, Tennessee 37830, USA
gallmeierfz@ornl.gov

Abstract - *The Inner Plug, and the Proton Beam Window Insert, central components of the SNS target monolith are exposed to high-level radiation fields during routine operation. The inner plug houses the SNS target, and the proton beam window insert contains the proton beam window located about 2 meters upstream from the target. Both the plug and the insert need to be replaced periodically due to radiation damage caused by high particle fluxes. In support of planning the replacement procedures, detailed information about residual radiation levels of the plug and insert components was requested as well as predictions of the radiation exposure to personnel during the change out. In addition shielding casks had to be designed for proper enclosure of the activated components.*

Analyses were performed to assess the dose rates for all steps of replacement. The analyses were performed in three steps. Firstly, transport calculations were performed to assess the isotope production rates in the zones. Secondly an activation analysis generated the resulting decay gamma sources for all cells of the complex 5 meters thick SNS target monolith structures. Third, decay gamma sources were used in subsequent transport analyses of the dose rates for all change out steps including the determination of the required shielding casks for the reusable plug components and the components which will be replace. This paper will present details of the analyses and the results.

I. INTRODUCTION

At Oak Ridge National Laboratory a Spallation Neutron Source[1] (SNS) is in construction, which will become a world class neutron scattering facility. A high intensity beam of 1 GeV protons generated in a linac[2] will direct 1.4 MW power to a liquid mercury target. Radiation damage of structural material exposed to the high proton beam current and the secondary radiation generated in interactions of the protons with materials force periodic replacement of key components, the target, the inner plug, which houses the target, and the proton beam window insert, which contains the proton beam window, located about 2 meters upstream from the target.

All these components will be highly activated and will have to be handled with care. Planning of the change out scenarios needs detailed information about the activity of the components and the residual gamma radiation fields. The target will be extracted directly into a hot cell and disassembled there, and is therefore not of concern here. The inner plug and the proton beam window insert are mounted through vertical shafts form top of the target shielding monolith. After removing the heavy shielding, the plugs and the inserts will be extracted into temporary shielding casks and moved to storage places.

II. METHODOLOGY OF THE CALCULATION

The typical sequence of the calculations was as follows. First, the MCNPX[3] calculation simulating the proton beam interaction with the proton beam window and the target was performed. This calculation provided neutron fluxes throughout the SNS target geometry, as well as nuclide production rates due to high-energy particles. Second, the calculation with OriHet95[4] was performed to determine the activation of the materials and the resulting gamma-ray emission rates. Third, the gamma-ray sources were put in the MCNPX model of the desired configuration and a transport of the gamma rays throughout the configuration was calculated, yielding

dose rates at desired locations by folding the gamma fluxes with flux-to-dose conversion coefficients.

All the transport calculations were performed with the MCNPX code version 2.1.5. This code was modified by extending the distributed computing capability to the high energy regime[5] using the Parallel Virtual Machine package, and by implementing an isotope production tally[6]. The first modification allows effectively performing a calculation on a cluster of computers, reducing the turnaround time of the calculation. The second enhancement provides isotope production rates from the physics model regime (high energy particles) directly in the MCNPX output rather than going the original route of generating and post-processing a high energy history file. Typical CPU times of the first step of calculation (protons on target) were 10-20000 minutes on a cluster of 1GHz Pentium-III machines using a LINUX operating system.

For the calculation of neutron fluxes and high energy production rates, the geometries typically extend 2-3 meters in radius and 6-7 meters in height. Typically large parts of the geometries consisted of steel shielding. As flux and isotope production data are required for all the shield plugs and also the shaft-near structure, variance reduction methods were heavily used to maintain a constant particle population throughout the geometry adjusted by the reduction of the particle weight for regions far from the target. After reaching an equilibrium spectrum the neutron flux drops with distance from the target following a simple exponential law. Hence it was the easiest to subdivide the bulk shielding into layers of equal thickness and to apply geometrical Russian roulette/splitting importance functions that were based on the changes of populations from a short "first shot" MCNPX run. A similar approach was applied for the shielding cask analyses that faced gamma transport through up to 40 cm of steel.

The intensity of activation and hence the decay gamma source strength drops rapidly with increased distances from the primary proton beam interaction zone. As a consequence, the low activity zones would be poorly sampled. Geometrical source biasing was the measure of choice to guarantee a constant source particle density throughout a structure with particle weights reflecting the source distribution.

The optimization of a shielding cask usually required several iterations of calculations. Firstly because although the locations of hot spots were obvious just by viewing the geometry, the intensities of the hot spots were not immediately guessed well. Secondly, interaction with mechanical engineers was needed to select the materials and to check weight limits due to fixed crane capacity. In order to save some CPU time, especially when the bulky inserts and shield blocks were analyzed, the gamma ray transport to the outer surface of the activated structure was performed only once, and the gamma ray surface source file was saved for subsequent calculations.

Various approaches were taken for scoring the dose rates in the shafts and outside the shield plugs. In some cases the dose rates were calculated in the volume corresponding to a 1.8 m, 70 kg man, modeled as an equivalent volume cylinder with length of 1.8 m and radius of 11.13 cm. Each cylinder was further divided into three equal-volume cells. At certain configurations, where achieving acceptable statistical errors was challenging, a ring (with height equal to the cylinder, but with much larger volume) was used instead of a cylinder to improve the scoring probability. In some cases the dose rates were scored on the surfaces of the casks and at a distance of 0.3 m from the cask. The cask surfaces were sometimes segmented to obtain a dose rate profile. Finally, some use was made of the mesh tally feature of the MCNPX code. Mesh tallies slow down the calculations a lot. For this reason we backed off from getting three-dimensional dose rate maps in geometries, but choose instead to obtain some two-dimensional dose rate slices through critical cuts of geometry.

The buildup and decay of the radioactive isotopes was calculated with the ORIHET95 code as laid out by Odano et.al.[7] The isotope production rates and hence the resulting decay gamma production rates, the code builds on, are in this approach cell averaged quantities. The geometry was therefore tailored into small pieces to achieve reasonable assessment of activity gradients. Off course this approach has its limits. On the one side unnecessary fragmentation of the geometry slows down the particle transport. Also more CPU resources are required converging the flux and isotope production rates in the smaller volumes. In addition, for each cell an activation buildup and decay calculations has to be performed, which is not so much a running time problem, but it boosts the amount of data produced and stored. On the other side, averaging over large volumes may smear out local peaks of activity, and as such underestimate local peaks of dose rates especially when streaming through gaps and slits generate peaks of activity near surface. Much guesswork on the split up of the geometry is asked from the analyst, to find a good balance of these two effects. The preparation of the isotope production rates from neutron fluxes, activation cross sections[8], and direct isotope production rate contributions from the spallation reactions is well automated by scripts, as well as the extraction and formatting of the decay gamma sources for the gamma transport calculations.

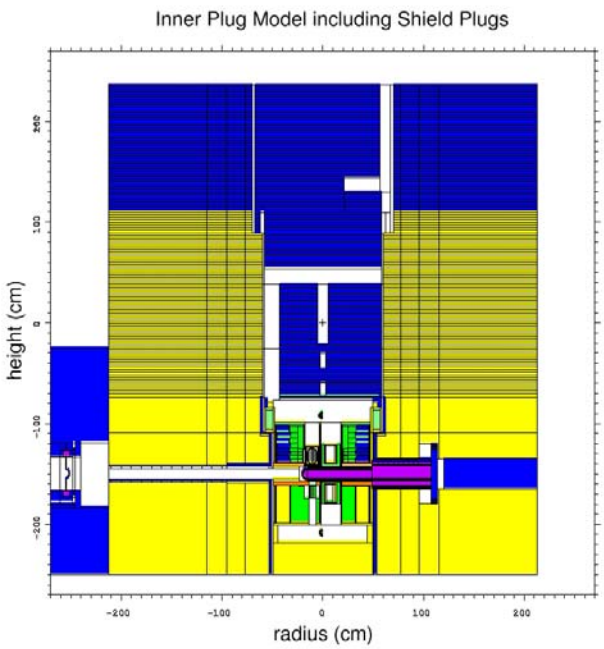

Fig. 1: Vertical cut through the SNS Inner Plug Model

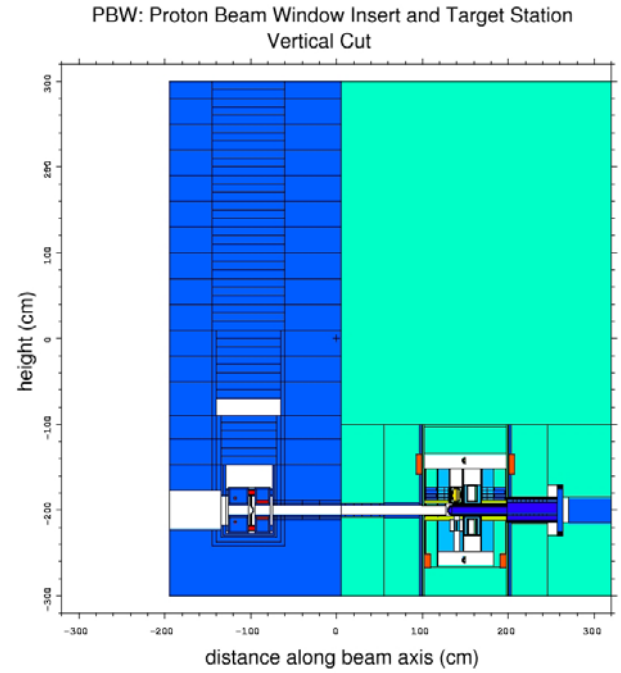

Fig. 2: Vertical cut through the proton beam window shaft and the inner plug housing the target.

The goal was to obtain dose rate values with relative standard deviations smaller than 1-3%. These standard deviations are only a small fraction of the overall uncertainty of the calculations. A major unquantifiable factor are the modeling compromises that in many cases did not allow to detail gaps and void zones, which may not be picked up adequately anyway by the particle transport. Also material description up to the trace elements may be crucial for the accurate activity buildup and decay and may increase some uncertainties. Especially the isotope production rates obtained from the high energy spallation reactions are in general predicted no better than a factor of 2 and in rare isotopes may be off one order of magnitude. The effect of smearing the activity and the resulting decay gamma source over cell volumes was already discussed earlier. Finally in none of the calculations neither β^+ nor β^- particles nor their secondary reaction products were considered, which neglects some fraction of the decay power. The calculated dose rates are believed to be within a factor of 2-3.

III. DETAILS OF INNER PLUG ANALYSES

The inner plug extends about 0.7 meters in radius and from 0.65 cm below the beam axis to about 2.3 meters above the beam axis. It houses the spallation target, four moderators on top and bottom of the target, a cylindrical beryllium neutron reflector around the moderators, and a steel reflector on the outside. Cutouts in the moderator planes allow the view of the moderator boxes through beam lines. The unit is carefully optimized for maximizing the neutron leakage into the neutron beam lines. The target is moved as an integral unit into the inner plug and is extracted prior to the exchange manipulations. The inner plug also includes an about 1.1 meters high steel plug on top of the reflector regions which has various holes and cutouts for coolant lines and for moderator supply.

For the inner plug activation calculations it was assumed that SNS operated at 2 MW for three years with the “realistic” beam-up beam-down schedule. The realistic operation schedule assumes that the SNS operates at full power for 1250 hours and is then shut down for a week. This is repeated four times, followed by the shutdown period till the end of the year. Such operation was simulated for three years. The gamma sources were taken in the third year of operation, 30 days after the fourth beam shutdown. The same activation scenario was used for all cells of the geometry. Hence the results presented are valid only for the first inner plug replacement. For later replacements the background gamma fluxes of the shaft and top shield plugs will be somewhat higher due to accumulated long-lived radionuclides. A 10 year activation period was used for the shield plugs on top of the inner plug.

IV. DETAILS OF PROTON BEAM WINDOW ANALYSES

The proton beam window at the target is the boundary between the high vacuum accelerator system and the helium atmosphere or rough vacuum environment of the target. About 2-3% of the incident proton beam undergoes nonelastic reactions and this contributes to the radiation field in this area. Neutron back-streaming from the target located at about 2.3 meter distance from the beam window also contributes to the radiation field. Hence it was felt of importance to model the proton beam window insert and the target environment as one entity as seen in Fig. 2. The activation analyses were performed for a cylindrical region with 1 meter radius extending from 1 meter below beam axis up to 5 meters above beam axis.

Although the proton beam window insert is expected to be replaced on a yearly basis, the radio nuclide inventory build up of the insert was in a conservatively manner calculated for a 2 year operations period of 5000 hours per year. The activation was performed in one time period without shutdown periods and is hence again conservative. Because the shield plugs are life of the facility components as well as the shaft including the monolith shielding, for these components an activity buildup time of 30 years was assumed, again performed in one long irradiation period. Furthermore it was assumed that the top shield plug will be extracted after 1 day of shutdown and the remainder of the plugs including the proton beam window insert will be extracted 5 days after shutdown.

V. INNER PLUG RESULTS

The configurations investigated are presented here in the chronological order of the inner plug replacement scenario.

The inner plug is intended to be replaced latest after three years of operation in the long shutdown period following four 1250 hour operation cycles with a one week service period in between. After a 30-days-long cool-down period the top shield layers are removed and allow access to the supply line (see Fig. 3). In detectors at locations 1-3 the radiation exposure of a man standing on top of the inner plug shield plugs was simulated, as well as the exposure of a man standing on top at the edge of the shaft. The dose rates at these positions, compiled in Table I, are moderate on top of the shield plugs and marginal at the edge of the shaft. This simulation does not include radiation from water lines, which are prone to show decay gammas from Be-7 plate-out on the inner wall surfaces and may be the dominating source.

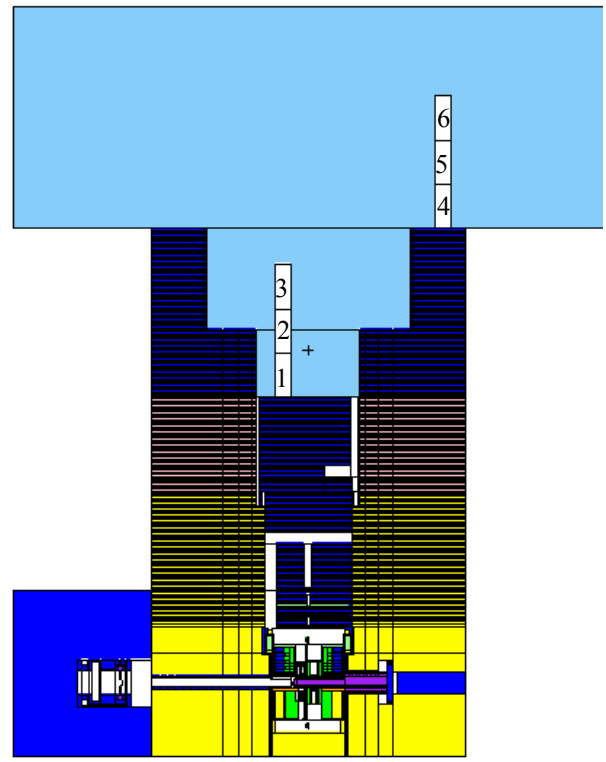

Fig. 3: Inner plug model with inserted inner plug and bottom and middle shield plugs. The top shield plugs are removed. Detector positions 1-6 are defined.

Table I: Dose rates in detector positions corresponding to Fig. 3.

Detector	Dose rate (mrem/h)	Rel. Standard Deviation
1	8.69	0.009
2	4.48	0.014
3	1.74	0.024
4	0.055	0.116
5	0.144	0.079
6	0.098	0.101

Next an alignment frame is inserted at the top of the shaft, and the upper and middle shield plugs are extracted into shielding casks. The plugs were assumed to be irradiated for 10 years of 2 MW operations. The doses rates at the outer surface of the shielding cask were calculated for three cases of wall thickness for the middle plug (1 cm, 6 cm, and 12 cm) and for two cases of wall thickness for the upper shield plug (1 cm and 10 cm) 30 days after shut-down. The model geometries and dose

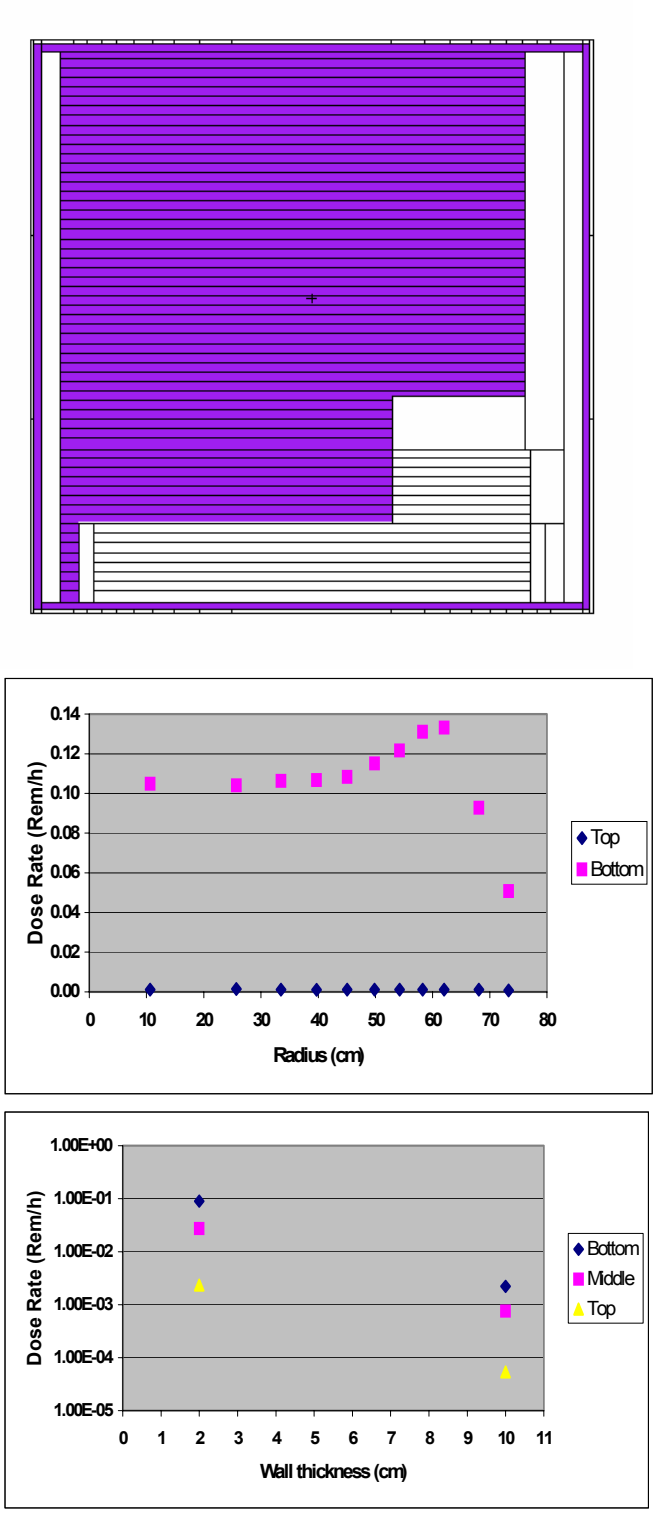

Fig. 4: Geometry of the upper shield plug in a shield cask; the radial dose rate profile on top and on the bottom at the outside of the 2-cm-thick shielding cask wall; and the dose rates outside the cylindrical cask walls averaged over the top, middle and bottom third of the cask wall height, for 2 cm and 10 cm wall thicknesses.

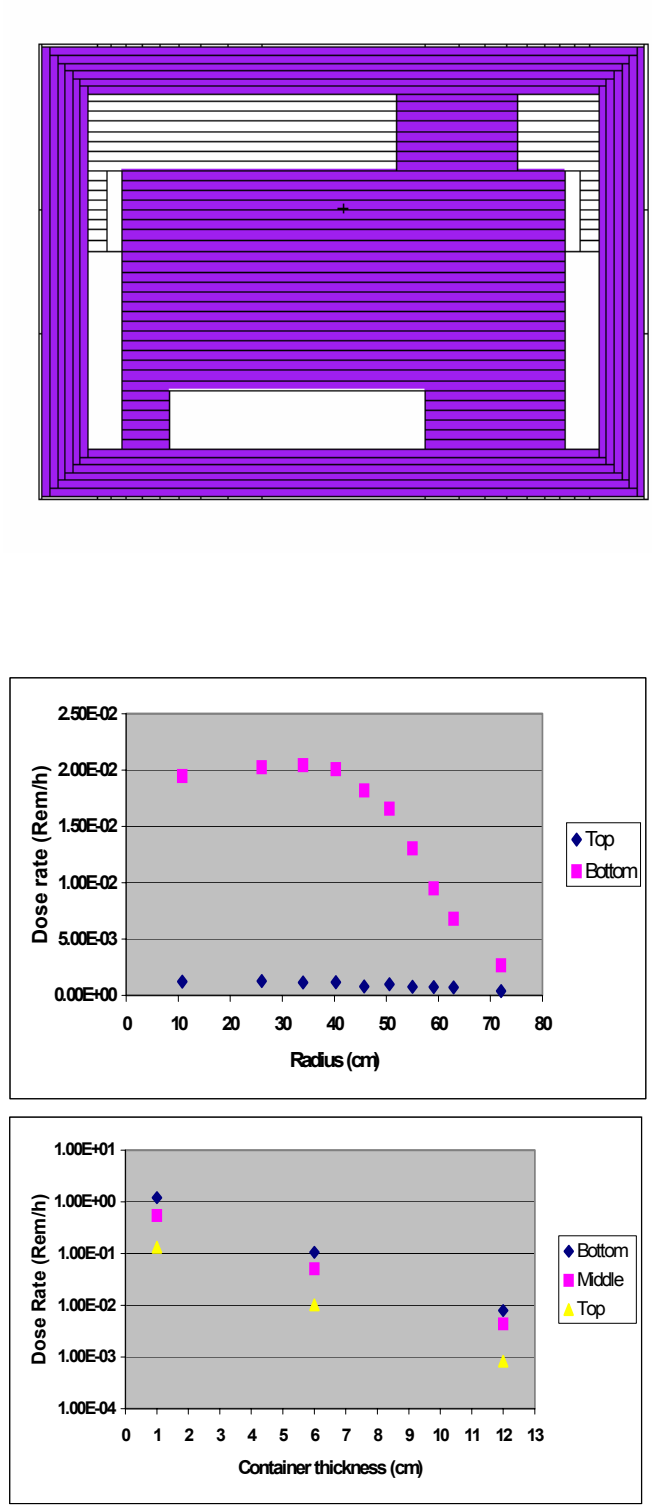

Fig. 5: Geometry of the middle shield plug in a shielding cask; the radial dose rate profile on top and on the bottom of at the outside of the 12-cm-thick shielding cask wall; and the dose rates outside the cylindrical cask walls, averaged over the top, middle, and bottom third of the wall height, for different wall thickness.

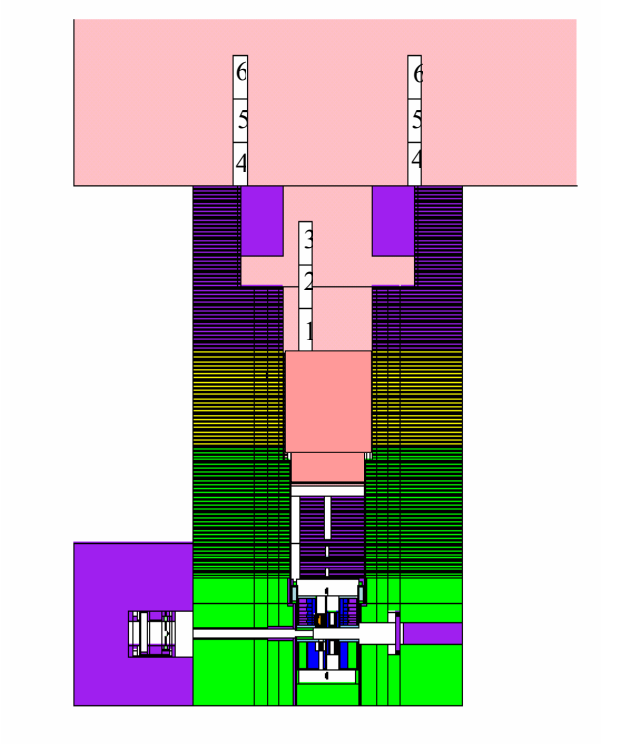

Fig. 6: Inner plug model with inserted inner plug, but upper and middle shield plugs removed. Detector positions 1-6 are defined with detectors 4-6 being cylinder rings.

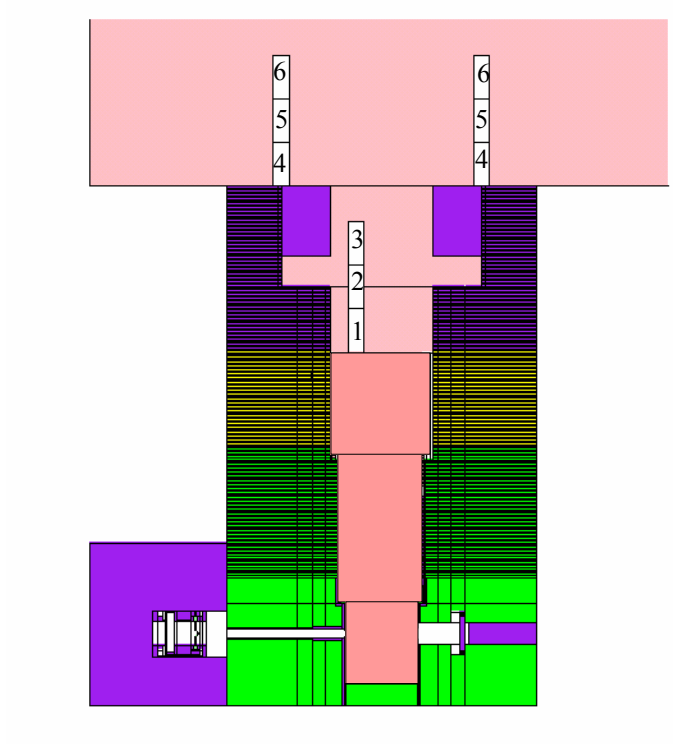

Fig. 7: Inner plug model with inner plug, and all shield plugs removed. Detector positions 1-6 are defined, with detectors 4-6 being cylinder rings.

Table II: Dose rates in detector positions corresponding to Fig. 6.

Detector	Dose rate (mrem/h)	Rel. Standard Deviation
1	2135	0.045
2	1734	0.050
3	1340	0.055
4	1.3	0.103
5	3.2	0.078
6	6.3	0.080

Table III: Dose rates in detector positions corresponding to Fig.7.

Detector	Dose rate (mrem/h)	Rel. Standard Deviation
1	49258	0.014
2	34941	0.016
3	25815	0.019
4	41.5	0.031
5	113	0.022
6	209	0.020

rates are presented in Fig. 4 and 5. The calculations show that for the upper shield plug 10 cm steel walls are sufficient as enclosure, for the middle shield plug 18 cm of steel will be required.

The extraction of the upper and middle shield plug increases the gamma shine from the highly activated inner plug structures to the top of the shaft as shown in Fig. 6. The dose rates at in-shaft positions and in positions at the edge of the shaft, as defined in Fig. 6, are listed in Table II. A worker leaning over the shaft would very likely be exposed to dose rates of 1 rem/hr, whereas at a location out of line of sight of the inner plug doses would be accumulated at a rate of several mrem/hr.

After extraction of the inner plug, the shaft is completely empty (see Fig. 7). The activated regions around the inner plug give rise to dose rates of 20 rem/hr for a lean-over location and still up to 0.2 rem/hr for a person out of line-of-sight near the shaft edge as detailed in Table III. The doses for this case are underestimated for inner plug replacements other than the first, because the calculation assumed an irradiation period of 3 years only. The shine can be easily reduced by a factor of 20 by closing the shaft with a 12-cm-thick steel lid.

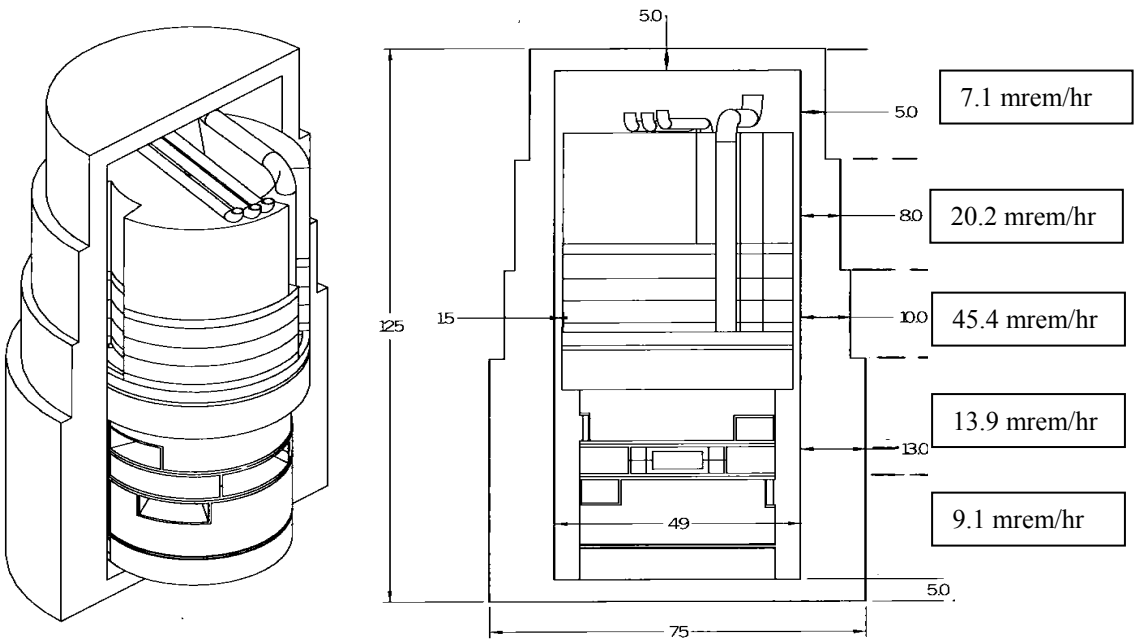

Fig. 8: Geometry of the inner plug insert and surface dose rates at the outside of the shielding cask. Some cask dimensions are given in inches.

The inner plug insert is extracted directly into a shielding cask, which is outlined in Fig.8. In the figure, surface dose rates at the outside of the shielding cask are given. The shielding cask is optimized with the crane limit of 50 tons in mind. At one meter distance from the cask the dose rates decrease to about 10 mrem/hr. At the hole on top of the cask for the reach-in of the crane, a dose of up to 3 rem/hr may be expected, leaving a maintenance worker handling the crane hook at a radiation field of 10-20 mrem/hr. Also pulling the inner plug to the top of the cask will produce an elevated radiation field of up to 80 mrem/hr at the outside of the cask, because of the steps in shield wall thickness. Lifting the loaded cask with open bottom will cause floor shine and much elevated dose rates. A 0.15 meters lift will cause a rise of the dose rates at 1 meter distance a level of 0.2 – 2 rem/hr depending of the elevation and floor material. A concrete floor was found to give a factor 2 higher doses rates compared to a steel floor. This means that shield walls and video systems will be required for handling of the cask.

VI. PROTON BEAM WINDOW RESULTS

The results of the calculations are presented in the order in which they appear during the extraction and replacement of the proton beam window insert. Geometry and dose rate information is plotted side by side for easier understanding.

The upper shield block (see Fig. 9) will be extracted 1 day after beam termination. It extends about one meter in height. The calculation demonstrated that both the contact dose rate and the dose rate at 0.3 meter distance are well below the regulatory limit of 0.25 mrem/hr.

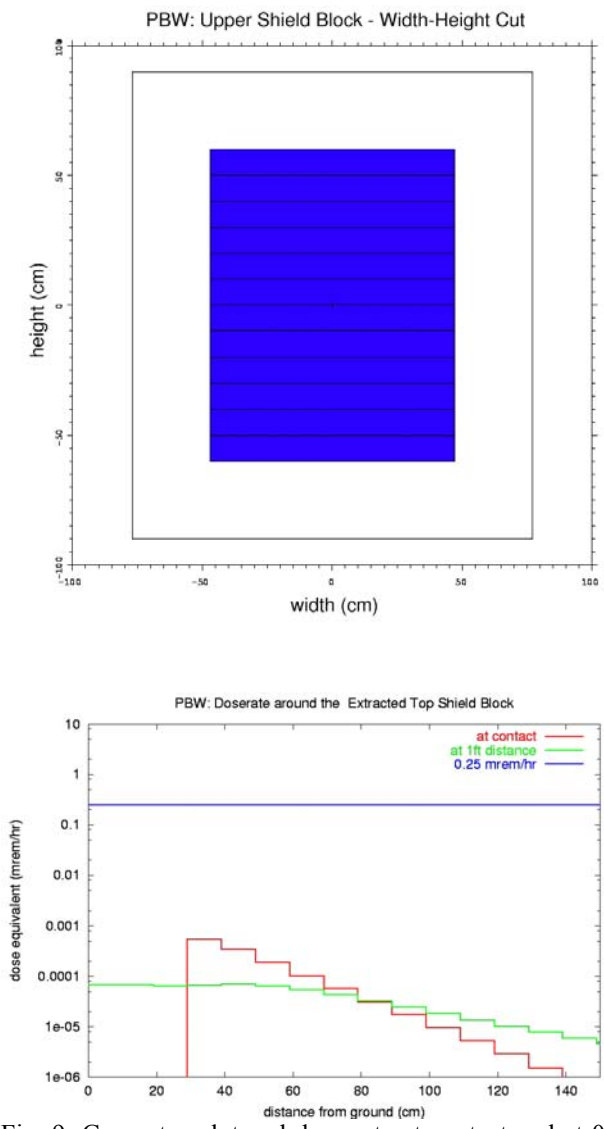

Fig. 9: Geometry plot and dose rate at contact and at 0.3 meter distance form the upper shield block.

The pieces down from the top shield plug may be extracted 5 days after beam termination. The additional four days of cool-down time are found to not help sufficiently to avoid a shielding cask for temporary storage of the middle shield plug. The wall thickness of the shielding cask varies from 20 cm steel on the bottom where the plug is hottest to 5 cm on the top (see Fig. 10). As some streaming paths along pipe chases were not considered in the model, which very likely will cause higher local activation a comfortable cushion was built into the cask design shielding-wise. The resulting dose rates outside are reported in the plots of Fig. 10. The casks are designed with an opening on top such that the hook of the high bay crane can reach through the cask and directly pull the shield blocks and the insert into their respective cask.

The bottom shield plug was found to require somewhat thicker steel wall for the cask (see Fig. 11) to attenuate the dose. The design finalized at 24 cm on the bottom and 20 cm on the sides and top. At the top, we expect dose levels of 10 mrem/hr shine through the hole for the crane hook that drop about a factor of three at 0.3 meter distance.

The proton beam window insert is a far more complex structure compared to the solid shield plugs; both form the mechanical and the gamma sources viewpoint (see Fig. 12). The proton beam windows insert moves up into a box shaped sleeve resting on top of the proton beam window box when the window is installed in its operation location. This sleeve is intended as a mechanical protection of the precision structures including vacuum flanges and acts as a first gamma shield at extraction of the insert. The window structure and the beam collimators are mounted hanging on a 60-cm-thick shield block, which is part of the insert. The most active component, by far, is the window itself, which is by its nature also the least inherently shielded component of the insert. It was found that the most about the gamma transport could be learned using mesh tally plots, because these identify local weaknesses of the cask shielding design. The local peaks of dose rates were identified and mitigated by lead inserts on the front and back side of the insert's beam openings and on the sides adjacent to the cooling channel ring. All lead inserts were integrated into the cask. Because of the crane limit of 50 tons, a compromise between mechanical and shielding design settled at cask walls of maximal 0.4 meters thickness, which allows local peaks of contact dose rates outside the shielding cask of several mrem/hr and doses of about 1 mrem/hr at 0.3 meters distance from the cask (see Fig. 13). A severe dose rate of about 1 rem/hr is expected at the opening for the crane hook on top of the cask.

Removing about 4 meters worth biological steel shielding leaves the proton beam window shaft open for shine of radiation (see Fig. 14), a maintenance worker might be exposed to looking down from the high bay. With the proton beam window insert still in place, dose rates of up to 100 mrem/hr can be expected. The extraction of the proton beam window insert results in a gamma shine of up to 3 rem/hr. Closing the shaft with a temporary lid is recommended.

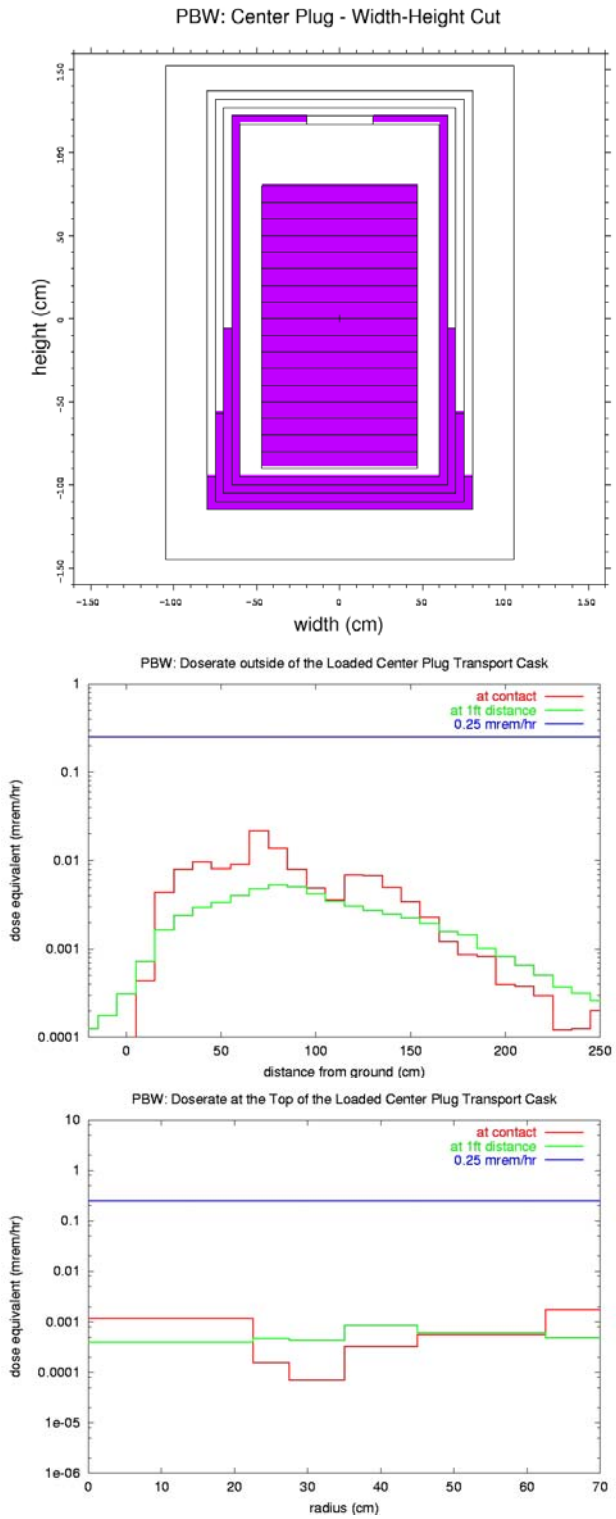

Fig. 10: Geometry plot and dose rate profiles outside the shielding cask containing the bottom shield block. Dose rate profiles are presented along the sides of the cask and on top of the cask.

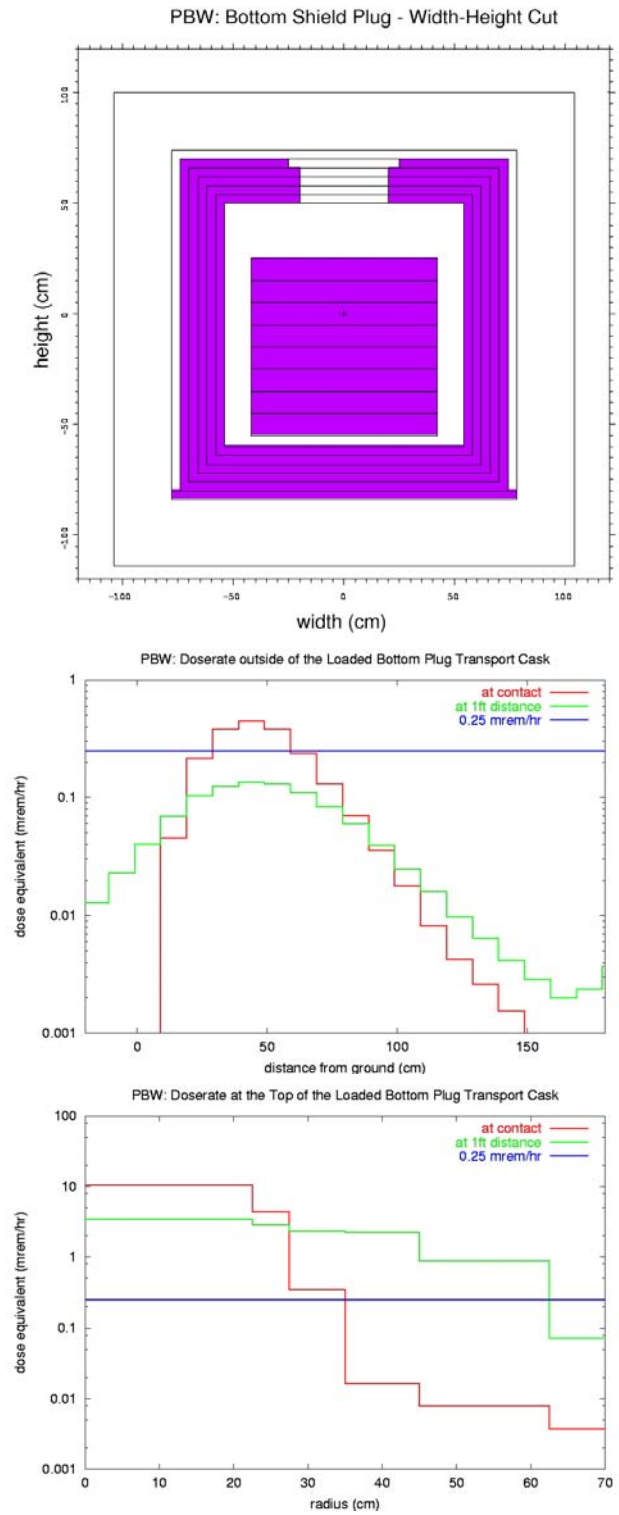

Fig. 11: Geometry plot and dose rate profiles outside the shielding cask containing the bottom shield block. Dose rate profiles are presented along the sides of the cask and on top of the cask.

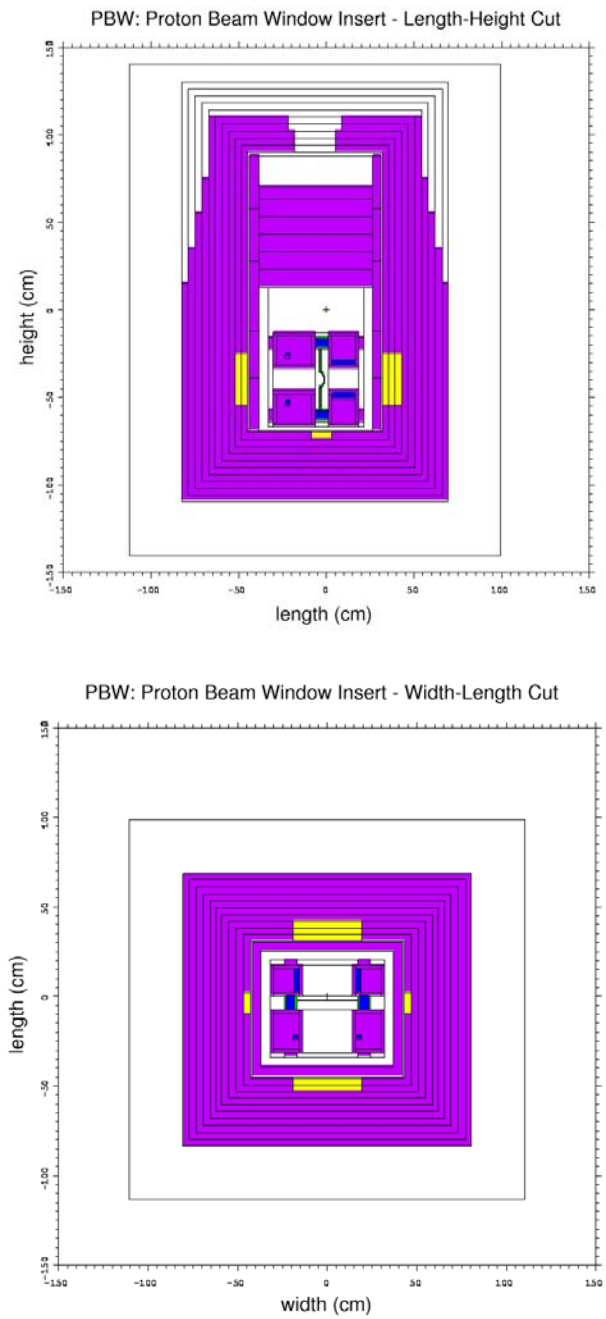

Fig. 12: Vertical and horizontal cuts through the proton beam window insert and the shielding cask at the beam opening.

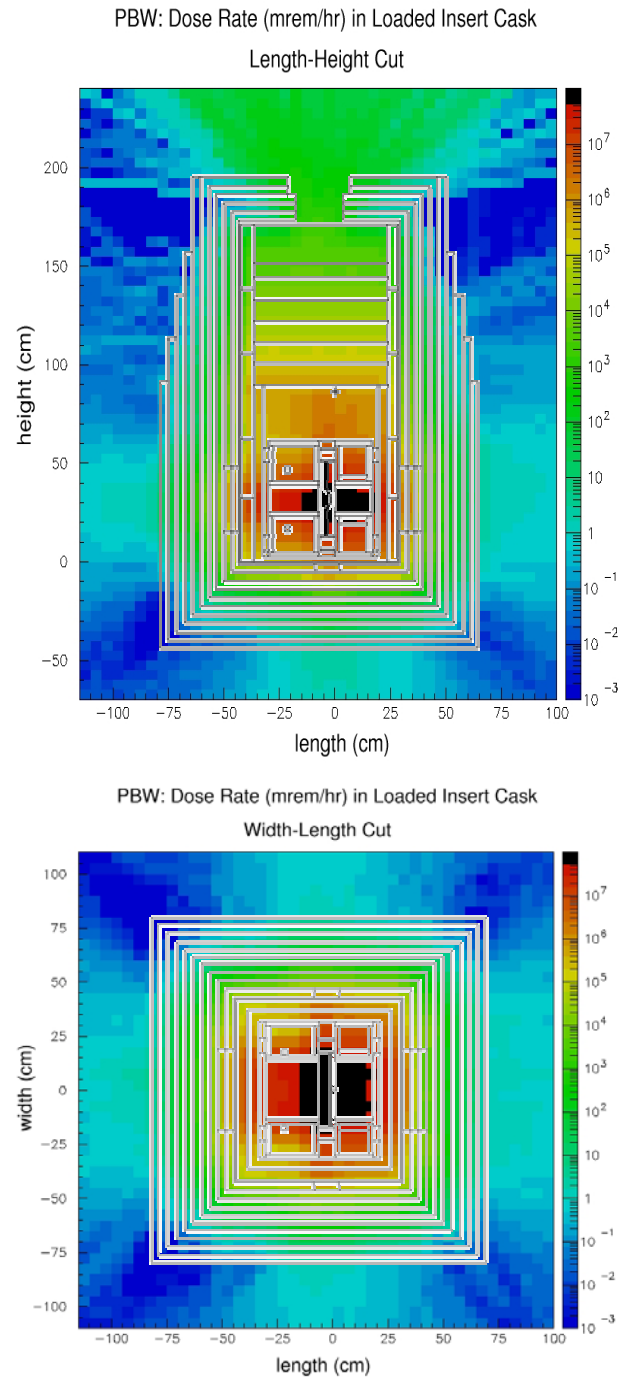

Fig. 13: Gamma dose rate maps for the proton beam window insert cuts presented in Fig. 12.

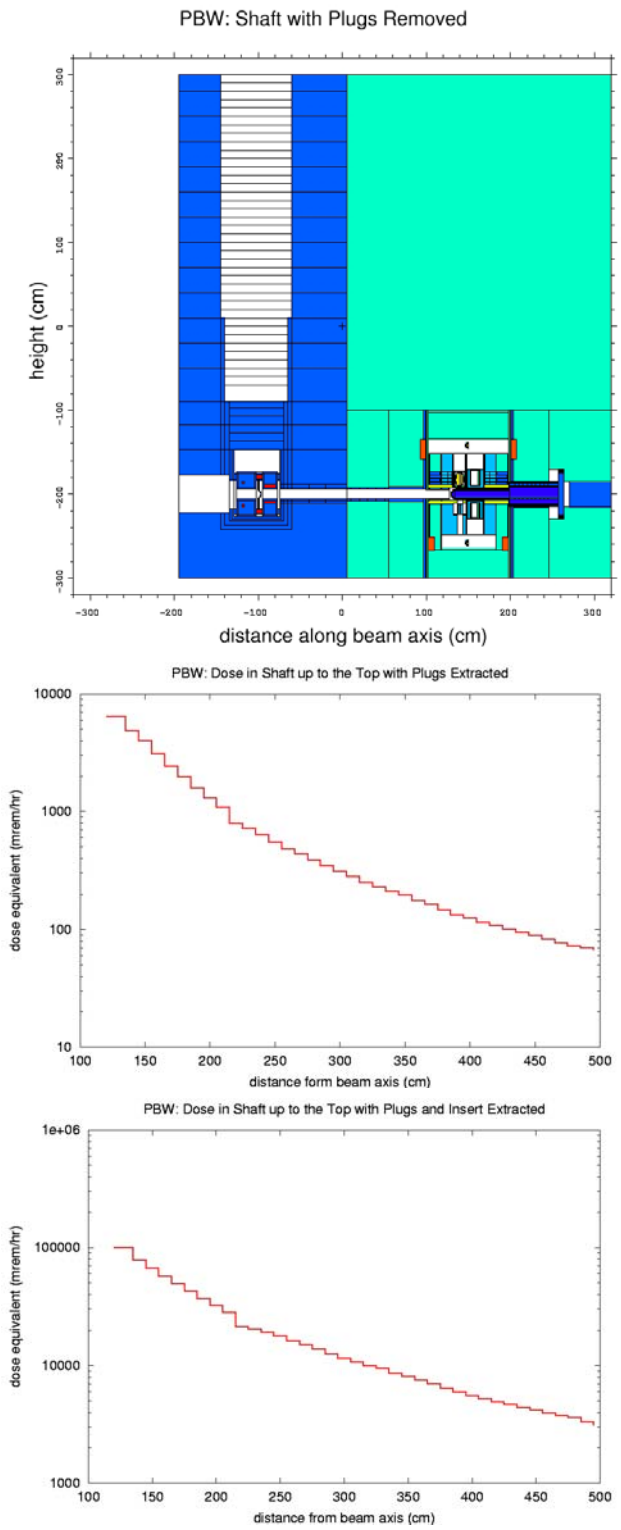

Fig. 14: Geometry of the proton beam window shaft with all shield plugs removed but with the insert still in the operating position Dose profiles are given for the case with the insert still in place, and the case of extracted insert.

VII. CONCLUSIONS

Particle transport and activation analyses have been performed to characterize the activities accumulating in the target components that need to be replaced periodically, as the inner plug and the proton beam window inserts. Shielding casks were designed for all activated components that need to be temporarily stored or replaced. Also dose maps were provided for the planning of the change-out scenarios.

VIII. REFERENCES

1. National Spallation Neutron Source Conceptual Design Report, Oak Ridge National Laboratory, NSNS/CDR-2/VI, 1997.
2. R. L. Kustom, "An overview of the Spallation Neutron Source Project", Proceedings of the XX International Linac Conference, Monterey, August 21-25 2000.
3. H. G. Hughes et. al., "MCNPX for Neutron-Proton Transport," International Conference on Mathematics & Computation, Reactor Physics & Environmental Analysis in Nuclear Applications, American Nuclear Society, Madrid, Spain, September 27-30, 1999.
4. P. Cloth et. al., "HERMES, A Monte Carlo Program System for Beam Material Interaction Studies," KFA Juelich, Report Juel-2203 (1988).
5. F. X. Gallmeier and P. D. Ferguson, "MCNPX Running Parallel under PVM", 12th Biennial Topical Meeting of Radiation Protection and Shielding, American Nuclear Society, Santa Fe, New Mexico, April 14-18, 2002.
6. F. X. Gallmeier, "Calculations of Operational and Residual Doses for the SNS Linac", Topical Meeting on Accelerator Applications/Accelerator Driven Transmutation Technology Applications '01, American Nuclear Society, Reno, Nevada, November 11-15, 2001.
7. N. Odano et al., "Development of the Activation Analysis Calculational Methodology for the Spallation Neutron Source (SNS)," 1998 ANS radiation Protection and Shielding Division Topical Conference, American Nuclear Society, Nashville, Tennessee, April 19-23, 1998; and Greg McNeilly, "AAS-Activation Analysis System", SNS-101040200-TR0003R00, UT-Battelle (1999).
8. A. B. Pashchenko and P. K. McLaughlin, "FENDL/A-1.1, Neutron Activation Cross Section Data Library for Fusion Applications," IAEA-NDS-148, Rev. 2 (1995).